Solid State Communications 151 (2011) 276–279

Contents lists available at ScienceDirect

Solid State Communications

journal homepage: www.elsevier.com/locate/ssc

High-pressure Raman spectroscopic studies on orthophosphates $Ba_3(PO_4)_2$ and $Sr_3(PO_4)_2$

Shuangmeng Zhai [a,*], Ang Liu [b], Weihong Xue [a], Yang Song [b]

[a] Key Laboratory of Orogenic Belts and Crustal Evolution, MOE; School of Earth and Space Sciences, Peking University, Beijing 100871, China

[b] Department of Chemistry, The University of Western Ontario, London, Ontario N6A 5B7, Canada

ARTICLE INFO

Article history:
Received 20 September 2010
Received in revised form
16 November 2010
Accepted 7 December 2010
by R. Merlin
Available online 13 December 2010

Keywords:
A. Orthophosphates
C. Raman spectroscopy
E. Vibration

ABSTRACT

By using diamond anvil cell (DAC), high-pressure Raman spectroscopic studies of orthophosphates $Ba_3(PO_4)_2$ and $Sr_3(PO_4)_2$ were carried out up to 30.7 and 30.1 GPa, respectively. No pressure-induced phase transition was found in the studies. A methanol:ethanol:water (16:3:1) mixture was used as pressure medium in DAC, which is expected to exhibit nearly hydrostatic behavior up to about 14.4 GPa at room temperature. The behaviors of the phosphate modes in $Ba_3(PO_4)_2$ and $Sr_3(PO_4)_2$ below 14.4 GPa were quantitatively analyzed. The Raman shift of all modes increased linearly and continuously with pressure in $Ba_3(PO_4)_2$ and $Sr_3(PO_4)_2$. The pressure coefficients of the phosphate modes in $Ba_3(PO_4)_2$ range from 2.8179 to 3.4186 cm^{-1} GPa^{-1} for ν_3, 2.9609 cm^{-1} GPa^{-1} for ν_1, from 0.9855 to 1.8085 cm^{-1} GPa^{-1} for ν_4, and 1.4330 cm^{-1} GPa^{-1} for ν_2, and the pressure coefficients of the phosphate modes in $Sr_3(PO_4)_2$ range from 3.4247 to 4.3765 cm^{-1} GPa^{-1} for ν_3, 3.7808 cm^{-1} GPa^{-1} for ν_1, from 1.1005 to 1.9244 cm^{-1} GPa^{-1} for ν_4, and 1.5647 cm^{-1} GPa^{-1} for ν_2.

1. Introduction

Alkaline earth metal orthophosphates, such as $Ba_3(PO_4)_2$ and $Sr_3(PO_4)_2$, are important substances for photoluminescence when they are doped with Eu^{2+} or Yb^{2+} [1–5]. In earth science, the orthophosphates of strontium and barium have been reported to be isomorphous with orthovanadates and orthoarsenates of the same alkaline earth elements [6–8]. On the other hand, γ-$Ca_3(PO_4)_2$, a typical analog of $Ba_3(PO_4)_2$ and $Sr_3(PO_4)_2$, has been named as tuite, and regarded as an important host for very large lithophile elements and rare earth elements in the upper mantle because it is one of the decomposed products of apatites [9–11]. The γ-$Ca_3(PO_4)_2$ is stable at least in the upper mantle [11], therefore, $Ba_3(PO_4)_2$ and $Sr_3(PO_4)_2$ may also be stable in the deep mantle as potential phosphorus hosts as well as rare earth elements.

The crystal analysis indicates that $Ba_3(PO_4)_2$ and $Sr_3(PO_4)_2$ are isostructural and rhombohedral in symmetry with the space group R-3m (No. 166, $Z = 3$) [6,12,13]. In the crystal structure (Fig. 1), a phosphorus atom is tetrahedrally coordinated by oxygen atoms and metal cations occupy two types of large metal sites. The Ba(1) or Sr(1) site has twelve oxygen neighbors and the Ba(2) or Sr(2) site is coordinated by ten oxygen atoms. The structure is characterized by the translationally interconnected polyhedral sequence PO_4–$M(2)O_{10}$–$M(1)O_{12}$–$M(2)O_{10}$–PO_4 (M = Ba or Sr) in the direction of the c axis [12].

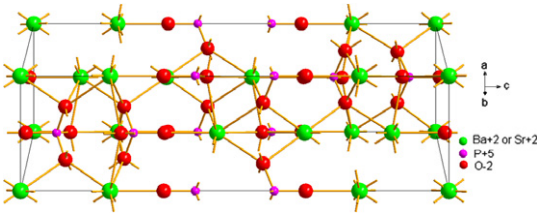

Fig. 1. The crystal structure of $Ba_3(PO_4)_2$ and $Sr_3(PO_4)_2$.

The physical properties of $Ba_3(PO_4)_2$ and $Sr_3(PO_4)_2$ at ambient conditions have been reported in literatures [14–16]. In previous studies [17,18], the physical properties of γ-$Ca_3(PO_4)_2$ under high pressure have been examined by in situ X-ray diffraction and Raman spectroscopy. However, the physical behaviors of the orthophosphates $Ba_3(PO_4)_2$ and $Sr_3(PO_4)_2$ at high pressure have not been investigated.

In the present work, we first characterize the *in-situ* Raman spectra of synthetic polycrystalline $Ba_3(PO_4)_2$ and $Sr_3(PO_4)_2$ at high pressure, using a diamond-anvil cell. The pressure effects on vibrations of $Ba_3(PO_4)_2$ and $Sr_3(PO_4)_2$ are also described.

2. Experimental

High-purity samples were prepared by solid-state reactions from $NH_4H_2PO_4$ and MCO_3 (M = Ba and Sr). Reagent-grade $NH_4H_2PO_4$ and MCO_3 (M = Ba and Sr) powders were mixed

* Corresponding author. Tel.: +86 10 62755631; fax: +86 10 62752996.
E-mail address: zhai@pku.edu.cn (S. Zhai).

0038-1098/$ – see front matter © 2010 Elsevier Ltd. All rights reserved.
doi:10.1016/j.ssc.2010.12.007

in the proportion corresponding to the $M_3(PO_4)_2$ (M = Ba and Sr) stoichiometry, and the mixture was ground sufficiently and pressed into pellets with a diameter of 5 mm under a uniaxial pressure of 30 MPa. The pellets were sintered at 1300 K for 48 h to form a single phase. The sintered product was ground finely and characterized by powder X-ray diffraction. The X-ray patterns confirmed the synthetic $Ba_3(PO_4)_2$ or $Sr_3(PO_4)_2$ is a single phase.

The high-pressure Raman measurements using a symmetric piston-cylinder type of DAC equipped with 400 μm culet diamond anvils were carried out with a customized Raman spectroscopy system. The experimental method used in this study was similar to a previous study [19]. A stainless steel plate with an initial thickness of 250 μm was used as a gasket. The central area of the gasket was pre-indented to a thickness of about 30 μm, and a hole of 150 μm in diameter was drilled at the center. The synthetic sample was loaded into the sample chamber, with the 16:3:1 methanol–ethanol–water as the pressure medium. A few ruby (Cr^{+3} doped α-Al_2O_3) chips as pressure markers were carefully placed inside the gasket sample chamber before the sample was loaded. The sample pressures were determined using the ruby fluorescence method with an accuracy of ±0.1 GPa [20]. Micro-Raman spectra were recorded in backscattering geometry using a SpectraPro Raman spectrometer from Acton with an ultra-sensitive, back-illuminated, liquid nitrogen cooled CCD detector. The resolution is better than 1 cm^{-1}. Excitation was achieved by adopting an argon-ion laser from Coherent Inc. with a wavelength of 488 nm and an output power of 0.350 W. The spectrometer was calibrated using a neon lamp achieving a spectral uncertainty of ±1 cm^{-1}. The acquisition time of each spectrum was 90 s.

3. Results and discussion

According to the factor group analysis based on the R-3m space group (D^5_{3d}), the $Ba_3(PO_4)_2$ and $Sr_3(PO_4)_2$ structures yield the same Raman active vibrations as the following:

$$\Gamma = 5A_{1g} + 6E_g.$$

Thus, a total of 11 Raman vibrational modes are predicted. Among these, the internal modes include two antisymmetric stretching ($A_{1g}+E_g$, ν_3), one symmetric stretching (A_{1g}, ν_1), two deformation bending (A_{1g} + E_g, ν_4) and one bending vibration (E_g, ν_2). The external vibrations include PO_4 translations (A_{1g} + E_g), Ba or Sr translations (A_{1g} + E_g) and PO_4 librations (E_g).

The Raman spectra of $Ba_3(PO_4)_2$ and $Sr_3(PO_4)_2$ at ambient conditions are shown in Fig. 2. The number of observed Raman vibrations is fewer than predicted, because of the low intensity of some external modes. In Fig. 2, six Raman active vibrations can be attributed to the phosphate internal modes. For $Ba_3(PO_4)_2$, the corresponding wavenumbers are 1043 and 980 cm^{-1} for ν_3 ($A_{1g}+E_g$), 929 cm^{-1} for ν_1 (A_{1g}), 601 and 563 cm^{-1} for ν_4 (A_{1g} + E_g), and 413 cm^{-1} for ν_2 (E_g). And for $Sr_3(PO_4)_2$, the corresponding wavenumbers are 1071 and 997 cm^{-1} for ν_3 ($A_{1g}+E_g$), 954 cm^{-1} for ν_1 (A_{1g}), 622 and 573 cm^{-1} for ν_4 ($A_{1g}+E_g$), and 418 cm^{-1} for ν_2 (E_g). The external modes deriving from the vibrations of PO_4 and Ba–O or Sr–O bonds below 400 cm^{-1} were observed at 207, 166 and 113 cm^{-1} for $Ba_3(PO_4)_2$, and at 244, 218, 174 and 143 cm^{-1} for $Sr_3(PO_4)_2$, respectively. These vibrations agree with previous Raman characteristics of $Ba_3(PO_4)_2$ and $Sr_3(PO_4)_2$ at ambient conditions [15,16]. The different Raman shifts between $Ba_3(PO_4)_2$ and $Sr_3(PO_4)_2$ for the same vibrations are mainly due to the interatomic distances which have been reported by previous studies [12,13], as listed in Table 1. The corresponding interatomic distances are smaller in $Sr_3(PO_4)_2$ than those in $Ba_3(PO_4)_2$. A smaller bond length implies a stiffer or stronger bond, i.e., large force constant, and consequently higher vibrational frequency according to Hooke's law, which is consistent with our observations in this study.

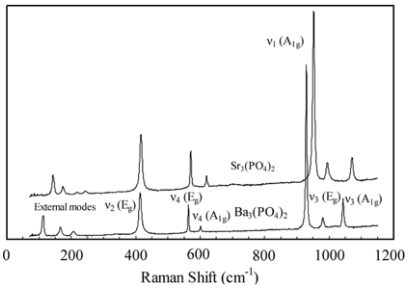

Fig. 2. Raman spectra of $Ba_3(PO_4)_2$ and $Sr_3(PO_4)_2$ at ambient conditions.

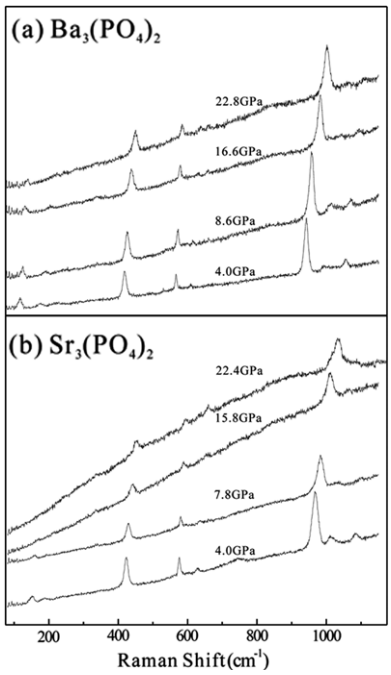

Fig. 3. Raman spectra of $Ba_3(PO_4)_2$ and $Sr_3(PO_4)_2$ under high pressures.

High-pressure Raman spectra of $Ba_3(PO_4)_2$ and $Sr_3(PO_4)_2$ were collected up to 30.7 GPa and 30.1 GPa, respectively. The typical Raman spectra of $Ba_3(PO_4)_2$ and $Sr_3(PO_4)_2$ at high pressures are reproduced in Fig. 3. It is obvious that, with increasing of pressure,

Table 1
Interatomic distances (Å) of $Ba_3(PO_4)_2$ and $Sr_3(PO_4)_2$, as well as γ-$Ca_3(PO_4)_2$.

	$Ba_3(PO_4)_2$		$Sr_3(PO_4)_2$		γ-$Ca_3(PO_4)_2$
	Ref. [12]	Ref. [13]	Ref. [12]	Ref. [13]	Ref. [10]
P–O(1)	1.542(8)	1.55(1)	1.522(6)	1.54(1)	1.526(6)
P–O(2) (×3)	1.549(2)	1.56(1)	1.549(2)	1.55(2)	1.535(2)
M(1)–O(1) (×6)	3.2354(3)	3.24(1)	3.1128(5)	3.14(1)	3.0359(4)
M(1)–O(2) (×6)	2.737(2)	2.74(2)	2.571(2)	2.58(1)	2.440(3)
M(2)–O(1)	2.636(8)	2.64(3)	2.435(6)	2.43(2)	2.239(5)
M(2)–O(2) (×3)	2.858(1)	2.89(2)	2.750(1)	2.69(1)	2.509(4)
M(2)–O(2) (×6)	2.906(2)	2.86(1)	2.686(2)	2.75(1)	2.686(2)

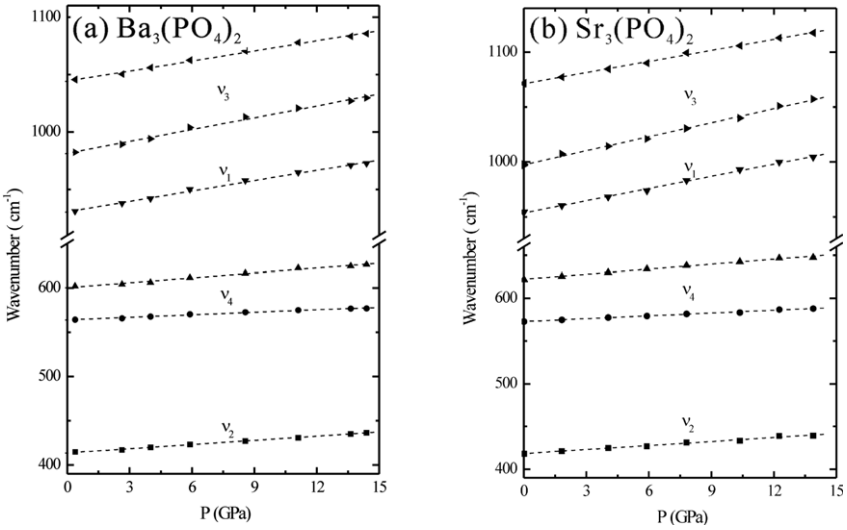

Fig. 4. Raman shifts of PO_4 internal modes as a function of pressure below 14.4 GPa in $Ba_3(PO_4)_2$ and $Sr_3(PO_4)_2$. The dashed lines represent the linear fittings of data.

the Raman peaks of $Ba_3(PO_4)_2$ and $Sr_3(PO_4)_2$ gradually shift to higher frequencies, which indicates a decreasing bond length of the phosphate tetrahedron and metal polyhedron. The spectra of $Ba_3(PO_4)_2$ and $Sr_3(PO_4)_2$ do not show any splitting or merging peaks, which indicates that no phase transformations occur in the present study.

In the present study, a methanol:ethanol:water (16:3:1) mixture was used as pressure medium, which remains hydrostatic up to 14.4 GPa at room temperature [21]. Therefore, the non-hydrostatic effect is inevitable for the pressure range of this study (up to 30 GPa). In order to avoid the non-hydrostatic effect, we only used the data collected below 14.4 GPa for quantitative analysis. The Raman shift *versus* pressure plots of $Ba_3(PO_4)_2$ and $Sr_3(PO_4)_2$ are illustrated in Fig. 4. It is noted that, due to the relatively low intensities of external vibrations of $Ba_3(PO_4)_2$ and $Sr_3(PO_4)_2$ during compression, it is difficult to determine the external modes under high pressures precisely. Therefore, the changes of external vibrations of $Ba_3(PO_4)_2$ and $Sr_3(PO_4)_2$ at high pressures are not considered in this study. The Raman shifts of PO_4 internal modes in $Ba_3(PO_4)_2$ and $Sr_3(PO_4)_2$ change linearly and continuously with pressure.

The pressure coefficients (α) of PO_4 modes in $Ba_3(PO_4)_2$ and $Sr_3(PO_4)_2$ (Table 2) indicate that ν_3 and ν_1 stretching vibrations in the high-frequency region are more sensitive to pressure compared to the ν_4 and ν_2 bending vibrations in the low-frequency region for the same composition. In fact, the pressure coefficients of ν_3 and ν_1 modes in $Ba_3(PO_4)_2$ are 2.8179–3.4186 cm^{-1} GPa^{-1} and 2.9609 cm^{-1} GPa^{-1}, and in $Sr_3(PO_4)_2$ are 3.4247–4.3765 cm^{-1} GPa^{-1} and 3.7808 cm^{-1} GPa^{-1}, whereas the coefficients for ν_4 and ν_2 modes in $Ba_3(PO_4)_2$ are 0.9855–1.8085 cm^{-1} GPa^{-1} and 1.4330 cm^{-1} GPa^{-1}, and in $Sr_3(PO_4)_2$ are 1.1005–1.9244 cm^{-1} GPa^{-1} and 1.5647 cm^{-1} GPa^{-1}, respectively.

In previous study, the high-pressure Raman spectra of γ-$Ca_3(PO_4)_2$, which has the same structure as $Ba_3(PO_4)_2$ and $Sr_3(PO_4)_2$, have been investigated [18]. The results are also listed in Table 2. Obviously, the wavenumbers of ν_{i0} and pressure coefficients (α) of corresponding PO_4 modes in γ-$Ca_3(PO_4)_2$ are lager than those in $Ba_3(PO_4)_2$ and $Sr_3(PO_4)_2$ except the ν_2 bending vibration. The differences are due to the different interatomic distances compared in Table 1. For the ν_2 bending vibration in γ-$Ca_3(PO_4)_2$, other factors, such as interatomic angles, may have a large effect.

The pressure coefficients of the different Raman modes can be used to obtain the Grüneisen parameters which are required in many theoretical calculations. However, there is no information for the isothermal bulk modulus of $Ba_3(PO_4)_2$ and $Sr_3(PO_4)_2$. Hence, the mode-Grüneisen parameters cannot be calculated in this study. Based on the fact that pressure coefficients of all PO_4 internal modes are smaller for $Ba_3(PO_4)_2$ than $Sr_3(PO_4)_2$, we may deduce a smaller compressibility for $Ba_3(PO_4)_2$ than $Sr_3(PO_4)_2$ under high pressure.

Table 2
Raman shifts of PO_4 modes in $Ba_3(PO_4)_2$ and $Sr_3(PO_4)_2$ with pressure. ν_{i0} and α represent the parameters in the expression: $\nu_P = \nu_{i0} + \alpha P$, where ν_P and ν_{i0} are in cm^{-1} and α is in cm^{-1} GPa^{-1}. The results for γ-$Ca_3(PO_4)_2$ [18] are listed for comparison.

PO_4 modes	$Ba_3(PO_4)_2$		$Sr_3(PO_4)_2$		γ-$Ca_3(PO_4)_2$ [18]	
	ν_{i0}	α	ν_{i0}	α	ν_{i0}	α
ν_3	1044.6	2.8179	1071.1	3.4247	1094.9	3.7227
	981.7	3.4186	997.0	4.3765	1003.8	4.9186
ν_1	930.0	2.9609	953.4	3.7808	978.8	4.3067
ν_4	600.5	1.8085	622.3	1.9244	641.6	2.1173
	563.6	0.9855	572.8	1.1005	576.8	1.1536
ν_2	414.0	1.4330	418.3	1.5647	412.2	1.5251

4. Conclusions

We first measured the Raman spectra of synthetic orthophosphates $Ba_3(PO_4)_2$ and $Sr_3(PO_4)_2$ up to 30.7 GPa and 30.1 GPa, respectively. The Raman shifts of all PO_4 internal modes increase linearly with pressure, and no pressure-induced phase transformation occurs in present studies. The pressure coefficients of phosphate modes of $Ba_3(PO_4)_2$ and $Sr_3(PO_4)_2$ were determined, and the pressure coefficients of corresponding modes are smaller for $Ba_3(PO_4)_2$ than $Sr_3(PO_4)_2$, indicating a relative softer compressibility for $Ba_3(PO_4)_2$ than $Sr_3(PO_4)_2$.

Acknowledgements

We thank the anonymous reviewer for helpful comments and suggestions, and Prof. Roberto D. Merlin for editorial handling. We are grateful to X. Wu for his helpful discussion. This work was financially supported by the NSFC (grant no. 40973045) and by a Discovery Grant, a Research Tools and Instruments Grant from the Natural Science and Engineering Research Council of Canada, a Leaders Opportunity Fund from the Canadian Foundation for Innovation and an Early Researcher Award from the Ontario Ministry of Research and Innovation.

References

[1] F.C. Palilla, B.E. O'Reilly, V.J. Abbruscato, J. Electrochem. Soc. 117 (1970) 87–91.
[2] J.R. Looney, J.J. Brown, J. Electrochem. Soc. 118 (1971) 470–473.
[3] S. Lizzo, E.P. Klein Nagelvoort, R. Erens, A. Meijerink, G. Blasse, J. Phys. Chem. Solids 58 (1997) 963–968.
[4] S.Z. Toma, J. Lumin. 31–32 (1984) 727–730.
[5] P. Dorenbos, J. Phys.: Condens. Matter 15 (2003) 2645–2665.
[6] W.H. Zachariasen, Acta Crystallogr. 1 (1948) 263–265.
[7] A. Durif, Acta Crystallogr. 12 (1959) 420–421.
[8] P. Süsse, M.J. Burger, Z. Krist. 131 (1970) 161–174.
[9] J.K. Murayama, S. Nakai, M. Kato, M. Kumazawa, Phys. Earth Planet. Inter. 44 (1986) 293–303.
[10] K. Sugiyama, M. Tokonami, Phys. Chem. Miner. 15 (1987) 125–130.
[11] X. Xie, M.E. Minitti, M. Chen, H.K. Mao, D. Wang, J. Shu, Y. Fei, Eur. J. Mineral. 15 (2003) 1001–1005.
[12] K. Sugiyama, M. Tokonami, Mineral. J. 15 (1990) 141–146.
[13] B. Manoun, L. Popović, D. de Waal, Powder Diffr. 18 (2003) 122–127.
[14] R.W. Mooney, S.Z. Toma, R.L. Goldsmith, J. Inorg. Nucl. Chem. 30 (1968) 1669–1675.
[15] M.E. Poloznikova, V.V. Fomichev, Russ. Chem. Rev. 63 (1994) 399–409.
[16] L. Popović, B. Manoun, D. de Waal, J. Alloys Compd. 343 (2002) 82–89.
[17] S. Zhai, X. Liu, S. Shieh, L. Zhang, E. Ito, Am. Mineral. 94 (2009) 1388–1391.
[18] S. Zhai, X. Wu, E. Ito, J. Raman Spectrosc. 41 (2010) 1011–1013.
[19] S. Xie, Y. Song, Z. Liu, Can. J. Chem. 87 (2009) 1235–1247.
[20] H.K. Mao, J. Xu, P.M. Bell, J. Geophys. Res. 91 (1986) 4673–4676.
[21] I. Fujishiro, G.J. Piermarini, S. Block, R.G. Munro, in: C.M. Backman, T. Johannisson, L. Tegnér (Eds.), High Pressure in Research and Industry, Arkitektkopia, Uppsala, 1982, pp. 608–611.